jth

ORIGINAL ARTICLE

Targeted SERPIN (TaSER): A dual-action antithrombotic agent that targets platelets for SERPIN delivery

Wariya Sanrattana[1] | Simone Smits[1] | Arjan D. Barendrecht[1] |
Nadine D. van Kleef[1] | Hinde El Otmani[1] | Minka Zivkovic[2] | Mark Roest[3,4] |
Thomas Renné[5,6] | Chantal C. Clark[1] | Steven de Maat[1] | Coen Maas[1]

[1]CDL Research, University Medical Center Utrecht, Utrecht University, Utrecht, The Netherlands

[2]Van Creveldkliniek, University Medical Center Utrecht, Utrecht University, Utrecht, The Netherlands

[3]Synapse Research Institute, Maastricht, The Netherlands

[4]Department of Biochemistry, Cardiovascular Research Institute Maastricht, Maastricht University, Maastricht, The Netherlands

[5]Institute for Clinical Chemistry and Laboratory Medicine, University Medical Center Hamburg-Eppendorf, Hamburg, Germany

[6]Center for Thrombosis and Hemostasis (CTH), Johannes Gutenberg University Medical Center, Mainz, Germany

Correspondence
Coen Maas, CDL Research, University Medical Center Utrecht, Utrecht University, Heidelberglaan 100, 3584 CX, Utrecht, the Netherlands.
Email: cmaas4@umcutrecht.nl

Abstract

Background: Occlusive thrombi are not homogeneous in composition. The core of a thrombus is rich in activated platelets and fibrin while the outer shell contains resting platelets. This core is inaccessible to plasma proteins. We produced a fusion protein (targeted SERPIN–TaSER), consisting of a function-blocking V_HH against glycoprotein Ibα (GPIbα) and a thrombin-inhibiting serine protease inhibitor (SERPIN; α1-antitrypsin $^{355}AIAR^{358}$) to interfere with platelet-driven thrombin formation.

Aim: To evaluate the antithrombotic properties of TaSER.

Methods: Besides TaSER, we generated three analogous control variants with either a wild-type antitrypsin subunit, a non-targeting control V_HH, or their combination. We investigated TaSER and controls in protease activity assays, (platelet-dependent) thrombin generation assays, and by western blotting. The effects of TaSER on platelet activation and von Willebrand factor (VWF) binding were studied by fluorescence-activated cell sorting, in agglutination studies, and in ATP secretion experiments. We studied the influence of TaSER in whole blood (1) on platelet adhesion on VWF, (2) aggregate formation on collagen, and (3) thrombus formation (after recalcification) on collagen and tissue factor.

Results: TaSER binds platelets and inhibits thrombin activity on the platelet surface. It blocks VWF binding and disassembles platelet agglutinates. TaSER delays tissue factor-triggered thrombin generation and ATP secretion in platelet-rich plasma in a targeted manner. In flow studies, TaSER interferes with platelet adhesion and aggregate formation due to GPIbα blockade and limits thrombus formation due to targeted inhibition of platelet-dependent thrombin activity.

Conclusion: The synergy between the individual properties of TaSER makes it a highly effective antithrombotic agent with possible clinical implications.

1 | INTRODUCTION

Platelets and thrombin are both key players in thrombus formation. Arterial thrombi contain a densely packed activated platelet core, where fibrin and thrombin are present at the base.[1-3] This core contains several prerequisites for efficient thrombin formation. In contrast, the outer shell of these thrombi is abundant with resting platelets and contains little, if any, fibrin. As integrin activation has not (yet) occurred in these platelets, it is likely that they are held together by von Willebrand factor (VWF) through glycoprotein Ibα (GPIbα). The core retains plasma proteins in a size-dependent manner.[4] Vice versa, it is largely inaccessible to thrombolytic agents.[5]

Serine protease inhibitors (SERPINs) regulate the activity of serine proteases by acting as a suicide substrate.[6] These molecules can be engineered to react with target proteases outside their natural scope. For example, an α1-antitrypsin variant (^{357}AIPM^{358} → ^{357}AIAR^{358}, α1AT-AIAR) was previously identified as an inhibitor of plasma kallikrein (Patent: US4973668A).[7,8] However, α1AT-AIAR is a broad-spectrum SERPIN that also inhibits thrombin (k_2: 5.5×10^4 M^{-1} s^{-1}; Table S1).[9] We hypothesized that targeted delivery of an antithrombotic SERPIN into a forming thrombus enhances its antithrombotic properties.

In this study, we engineered a targeted SERPIN (TaSER) by fusing α1AT-AIAR to a single-chain antibody fragment (V$_H$H) that binds to platelet GPIbα. In this way, we aimed to improve the antithrombotic potential of this SERPIN.

2 | MATERIALS AND METHODS

A complete list of reagents is provided in the supporting information.

2.1 | Construct design

2.1.1 | GPIbα-V$_H$H

Llama glama received four subcutaneous injections with recombinant GPIbα during a 4-week period. Twenty-four hours after the last injection, venous blood was collected from which peripheral blood lymphocytes were isolated by Ficoll gradient. Total RNA was isolated and transcribed into cDNA from which two V$_H$H genetic libraries in the *E. coli* TG1 strain (>10^7 diversity).[10] Recombinant GPIbα was immobilized overnight at 4°C on a 96-well Maxisorp plate. Phages were produced from the V$_H$H libraries overnight and isolated via polyethylene glycol (PEG; Mr = 6000) precipitation (20% m/v PEG6000 in 2.5 M NaCl). The coated microtiter plates and phages were blocked with 2% skimmed milk powder (m/v) in phosphate-buffered saline

Essentials

- We fused a platelet-targeting V$_H$H to a thrombin-inhibiting serine protease inhibitor (TaSER).
- The V$_H$H moiety targets platelet glycoprotein Ibα, inhibits von Willebrand factor binding, and disassembles platelet agglutinates.
- TaSER decreases platelet-dependent thrombin generation and delays platelet degranulation.
- TaSER limits thrombus buildup and fibrin formation in an *ex vivo* thrombosis model.

(PBS) for 1 h at room temperature (RT). Subsequently, phages were added to the coated microtiter plates and incubated for 2 h at RT. Microtiter plates were extensively washed with PBS-Tween (0.05% v/v), after which bound phages were eluted by adding 100 μl Triethylamine (0.1 M). After the elution, the pH was neutralized by the addition of 50 μl Tris (1 M, pH = 7.5). Isolated phages were added to exponentially growing *E. coli* TG1 for infection, after which infected bacteria were plated on Yeast Tryptone (YT)-agar plates containing (2% w/v) glucose and ampicillin (100 μg/ml) and incubated overnight at 37°C. Colonies were picked and grown as individual cultures in 2× YT media containing (2% w/v) glucose and ampicillin (100 μg/ml).

Next, V$_H$H protein sequences were codon-optimized for human expression via the web tool of Integrated Data Technologies (IDT). An *EcoRI* digestion site, followed by sequence encoding the tobacco etch virus (TEV) protease cleavage site (ENLYFQ/S) were placed upstream of the V$_H$H sequences.

For V$_H$H-fused α1-antitrypsin molecular cloning, a flexible linker region (SAAGGGGSGGGGSAAA), in which *PstI* and *BamHI* digestion sites were integrated, was placed downstream of the modified cDNA sequence of V$_H$H.

2.1.2 | α1-antitrypsin

The cDNA sequence of SERPINA1 that encodes α1AT-WT was obtained from the National Center for Biotechnology Information (NCBI) reference sequence (NM_001127707.1). The signal peptide sequence was replaced by an *EcoRI* digestion site and the TEV protease cleavage site. After the naturally occurring stop codon a *NotI* digestion site was placed. For the α1AT-AIAR construct, the modified cDNA sequence of SERPINA1 was mutated in which the nucleotide sequence encoding P2 and P1 residues was replaced with codons that encode alanine and arginine, respectively.

*Caplacizumab** The caplacizumab protein sequence (two identical V_HHs +AAA linker) was derived from the European Medicines Agency (EMA) assessment report (EMA/490172/2018; https://www.ema.europa.eu/en/documents/assessment-report/cablivi-epar-public-assessment-report_en.pdf). We designed a codon-optimized DNA sequence for expression in *E. coli* via the online tool of IDT. At the 5' end of this sequence, a *BamHI* digestion site was added and at the 3' end, a *NotI* digestion site was added.

2.2 | Cloning

*Caplacizumab** The construct was ordered as a double-stranded DNA fragment from IDT. The double-stranded DNA fragment was ligated into the pJET1.2 cloning vector. Caplacizumab* DNA was digested by *BamHI* and *NotI* and ligated into a modified pET32a+ expression vector (Merck-Millipore), containing a N-terminal PelB leader sequence, Hisx6 tag, and a TEV protease cleavage site. At the C-terminus, the V_HH is followed by a Myc tag and a stop codon.

The expression vector was transformed into BL21 pLysS *E. coli* and grown in 2× YT media containing 2% glucose, 100 µg/ml ampicillin, and 50 µg/ml chloramphenicol. Hereafter a 5 L fermentor containing ZYP-5052 autoinduction media (without trace metals) was inoculated and grown for 3 h at 37°C with 70% dissolved O_2. Hereafter, the temperature was lowered to 24°C and production continued overnight.

Bacteria were pelleted at $5000 \times g$ for 15 min and subsequently resuspended in binding buffer (25 mM HEPES, 500 mM NaCl, pH7.8) together with 1 mM $MgCl_2$ and 1 µg/ml DNAse. Bacteria were cracked by three freeze-thaw cycles using liquid nitrogen. Hereafter, samples were treated with lysozyme for 10 min at 37°C prior to centrifugation at $13,000 \times g$ for 60 min. Supernatant was collected and caplacizumab* was isolated using immobilized metal affinity chromatography. Caplacizumab* was further purified and buffer exchanged by gel filtration over a 75 pg HiLoad 26/600 Superdex column (Cytiva) prefilled with a 20 mM sodium citrate buffer (7% m/v sucrose, 0.01% v/v Tween 80, pH6.5). Protein concentration was determined by absorption at 280 nm and corrected for the extinction coefficient. Purity and degradation were assessed by Coomassie blue staining after sodium dodecyl sulfate polyacrylamide gel electrophoresis (SDS-PAGE).

2.2.1 | V_HH and α1-antitrypsin

All constructs were ordered as double-stranded DNA fragments from IDT and ligated into the pJET1.2 cloning vector. The ligated products were transformed into chemically competent TOP10 *E. coli*. Next, the amplified ligated products were digested and ligated into the pSM2 expression vector that encodes for an N-terminal Igκ secretion signal and double STREP-tag for protein purification.[10]

2.2.2 | V_HH-fused α1-antitrypsin

The V_HH-pSM2 plasmid (with the linker), as well as the SERPIN-containing pSM2 plasmid, was digested via *BamHI* and *NotI*. The SERPIN-encoding nucleotide sequence was inserted into the digested V_HH-pSM2 plasmid via T4 ligase. Construct sequences were confirmed by sequencing.

200 ml of HEK Freestyle cells (1.1×10^6 cells/ml) were transfected via 293Fectin (Thermo Fisher Scientific). After 24 h, 200 ml of fresh Freestyle culture media was added. Four days after transfection, supernatants were collected via centrifugation ($2000 \times g$ for 5 min). Supernatant was concentrated in STREP-buffer (100 mM Tris-HCL, 150 mM NaCl, 1 mM EDTA, pH = 8) via the QuixStand Benchtop system. V_HH-fused α1AT and variants were purified from the concentrate via strep-tactin Sepharose beads (IBA Lifesciences). Purified α1AT was dialyzed (4 mM sodium-acetate, 150 mM NaCl, pH = 5.4) and stored at −80°C. Protein concentrations were determined by α1AT ELISA (R&D Systems). Purity was assessed via 4%–12% Bis Tris-PAGE gel and Coomassie blue staining.

2.3 | Platelet-rich plasma and isolated platelet preparation

Whole blood from healthy donors (under approval of the local Medical Ethical Committee of the University Medical Center Utrecht) were collected in sodium citrated collection tubes on the day of experiments. Platelet-rich plasma (PRP) was separated via $160 \times g$ centrifugation for 15 min and subsequently collected. Platelet count was determined by CELL-DYN Emerald hematology analyzer (Abbott). The remaining blood product was further spun down at $2000 \times g$ for 15 min to separate platelet-poor plasma (PPP). Next, platelet count in the PRP was adjusted to $\pm 200 \times 10^9$/L by diluting with PPP of the same donor. For isolated platelet preparation, citrate-dextrose solution (ACD, 8.5 mM tri-sodium citrate, 7.1 mM citric acid, 11.1 mM D-glucose) was added to the undiluted PRP before centrifugation at $400 \times g$ for 15 min. The supernatant was removed, subsequently the pellet was resuspended back to the original volume in HEPES Tyrode buffer (HT buffer; 145 mM NaCl, 5 mM KCl, 0.5 mM Na_2HPO_4, 1 mM $MgSO_4$, 10 mM HEPES, 5.55 mM D-glucose, pH 6.5). PGI_2 (10 ng/ml final concentration) was added to the platelet suspension before another centrifugation at $400 \times g$ for 15 min. The supernatant was removed. The pellet was resuspended in HT buffer (pH 7.3) and platelet count was adjusted to $\pm 200 \times 10^9$/L.

2.4 | SDS-PAGE and western blotting

Samples were diluted in 3× sample buffer (SB; 30% glycerol, 0.18 M Tris-HCl, 6% SDS, Bromophenol blue, with or without 25 mM DTT for reduction), after which they were heated for 10 min at 95°C.

Samples were separated on 4%–12% Bis-Tris gels at 165 V for 65 min in MOPS buffer and transferred to Immobilon-FL membranes at 125V for 55 min in blotting buffer (25 mM Tris, 192 mM glycine, 20% (v/v) ethanol). Membranes were blocked for 2 h at RT with blocking buffer (Odyssey blocking reagent diluted 1:1 in TBS). Target proteins were detected by overnight incubation (at 4°C) of membranes with freshly prepared primary antibodies (Table S3). Membranes were washed with 0.05% (v/v) Tween in TBS (TBS-T), and primary antibody was detected with corresponding secondary antibody for 1 h at RT. Membranes were washed with TBS-T and analyzed on a near infrared Odyssey scanner (LI-COR). Band densitometry was analyzed with Odyssey software (LI-COR).

2.5 | Thrombin generation assays

2.5.1 | Protease activity assay

Purified thrombin (17.7 nM) and construct variants, α1AT-AIAR or vehicle (final concentration: 18.8–300 nM) were incubated (in 0.2% [w/v] BSA-HBS, pH = 7.4) for 5 min at 37°C in a 96-well assay plate. Hereafter, I1140 (Gly-Gly-Arg-AMC) fluorogenic substrate was added and conversion (ext: 380 nm em: 460 nm) was monitored for 30 min at 37°C.

2.5.2 | Thrombin generation assay (TGA)

Thrombin generation was performed as published.[11] Briefly, 60 µl of normal pooled plasma was incubated with 20 µl the construct variant in 0.2% BSA-HBS (final concentration: 9.38–600 nM) or vehicle at 37°C for 5 min. Hereafter 20 µl activator was added (4 µM phospholipid vesicles and 0.1 pM TF). Coagulation was initiated by the addition of 10 µl FluCa (17.5 mM HEPES, 16.67 mM CaCl$_2$, 0.42 mM Gly-Gly-Arg-AMC, 5.25% BSA, pH = 7.4). Fluorescence was read (ext: 380 nm em: 460 nm) and monitored for at least 90 min at 37°C. For calibration, the construct was replaced by 0.2% BSA-HBS and the activator was replaced by 20 µl thrombin-α2macroglobulin complex (Thrombin calibrator). The obtained data were converted into thrombin generation peaks via the Thrombinoscope software (Synapse). To assess platelet-dependent thrombin generation, TGA was performed in PRP in the presence of 1.5 µM corn trypsin inhibitor (CTI). The assay was performed as described for TGA in normal pooled plasma except that only 0.1 pM TF was added as an activator.

2.6 | Platelet binding studies

2.6.1 | Platelet pull down

500 µl PRP (in the presence of 1.5 µM CTI) from a healthy donor was incubated with 500 µl the construct (final concentration: 0,

9.38, 37.5, or 600 nM) for 10 min at 37°C. Next, ACD (8.5 mM tri-sodium citrate, 7.1 mM citric acid, 11.1 mM D-glucose) was added to the sample and platelets were isolated via 2000 × *g* centrifugation for 10 min. 200 µl supernatant was discarded. Platelet pellet was washed with 10 ng/ml PGI2 in HT buffer (pH 6.5) and spun down again at 2000 × *g* for 10 min. Hereafter, the pellet was resuspended in 45 µl non-reduced 3×SB for platelet samples. The presence of the construct was analyzed by western blotting.

2.6.2 | Platelet binding in fluorescence-activated cell sorting (FACS)

Serial dilution of 50 µl of construct variants (9.38–600 nM in 20 mM sodium citrate buffer; 7% m/v sucrose, 0.01% v/v Tween 80, pH6.5) or vehicle was preincubated in 5 µl of isolated platelets (±200 × 10^9/L) for 20 min at RT. Hereafter, samples were fixed with 500 µl formaldehyde (0.4% w/v) for 10 min at RT, centrifuged at 400 × *g* for 15 min. Supernatant was discarded. Platelet pellet was resuspended in 50 µl sheep anti α1AT polyclonal antibody (1:1000 dilution in HBS) and incubated at RT for 45 min. The sample was fixed again with 500 µl formaldehyde (0.4% w/v) for 10 min at RT. Platelets were centrifuged at 400 × *g* for 15 min. Supernatant was discarded. Platelet pellet was resuspended in 50 µl FITC conjugated rabbit anti-sheep antibody (1:80 dilution in HBS). After 45 min the sample was diluted in 200 µl of formaldehyde (0.4% w/v) and the samples were analyzed on a fluorescence-activated cell sorting (FACS) Canto II using FACS Diva software version 8.0.1.

2.6.3 | VWF competition binding in FACS

25 µl construct (9.38–600 nM in HT buffer pH 7.3) or vehicle was incubated with 5 µl citrated whole blood (1:6 dilution) for 20 min in FACS tubes. This dilution is needed to prevent platelet agglutination, which interferes with FACS analysis. Next, 25 µl ristocetin (880 µg/ml in HT buffer pH 7.3) was added and incubated for another 20 min. Five hundred µl of 0.4% PFA fixative was added to the samples and incubated for 10 min. The samples were spun down at 350 × *g* for 15 min, subsequently supernatants were discarded. VWF binding was detected by FITC conjugated-polyclonal sheep anti-human VWF antibody (20 µg/ml). Samples were fixed with 500 µl of 0.4% PFA and incubated for 10 min. The fixed sample was further diluted 1:1 in fixative, after which samples were analyzed on a FACS Canto II using FACS Diva software version 8.0.1. Platelets were gated based on their forward and sideward scatter. The median fluorescence intensity (MFI) of 5000 gated platelets was determined.

2.6.4 | Platelet agglutination

Platelet master mix was prepared by mixing isolated platelet suspension with 0.55 µg/ml iloprost, 0.28 mM RGDW, and 6.9 µg/ml VWF;

217.4 µl master mix was prewarmed for 5 min at 37°C in aggregrometer (CHRONO-LOG® Model 700, Chrono-log Corp.) where the mix was constantly mixed by a magnetic stirrer. Samples' baselines were calibrated against HT buffer. One min after, 0.79 mg/ml ristocetin was added to the master mix. After 6 min incubation, 600 nM construct (in HT buffer pH 7.3) was added to the mix. Light transmission was measured for 60 min; 143 nM Caplacizumab* was included as a positive control.

2.7 | Platelet function studies

2.7.1 | Platelet ATP secretion

In the presence of 1.5 µM CTI, whole blood obtained from healthy donor was mixed with the construct (9.38–600 nM; in 0.5% [w/v] 10 mM HEPES, 150 mM NaCl, 1 mM $MgSO_4 \cdot 7H_2O$, 5 mM KCl, 0.49 mM $MgCl \cdot 6H_2O$ pH = 7.4) or vehicle at 37°C in a U-bottom white 96-well plate. Afterward, a luminescence mix (8 µg/ml luciferase and 1 mM luciferin) was added. Platelet activation was initiated by adding 0.1 pM TF and 5 mM $CaCl_2$. Luminescence was read (all wavelengths) and monitored for 90 min at 37°C.

2.7.2 | Platelet activation in FACS

Serial dilution of 50 µl of constructs (0–600 nM), 0.9 U/ml thrombin, and 1:250 dilution of an in-house made Alexa647 conjugated anti-P-selectin-V_HH was preincubated with 5 µl of isolated platelets for 20 min at RT. Hereafter, samples were fixed with 500 µl formaldehyde (0.4% w/v) for 10 min at RT. Subsequently, the samples were analyzed for Alexa647 signal on a FACS Canto II using FACS Diva software version 8.0.1.

2.8 | Construct:thrombin complex formation on the platelet surface.

One hundred twenty-five µl PRP (in the presence of 1.5 µM CTI) from healthy donor was incubated with 25 µl construct (final concentration: 300 nM), 12.5 µl TF (0.1 pM), and 20 µl GPRP (8 mM) for 10 min at 37°C in HBS buffer. Hereafter prewarmed $CaCl_2$ solution was added (final concentration 16.67 mM) and incubated for 90 min at 37°C. After the incubation, 150 µl of sample was taken and mixed in 75 µl 3× non-reduced sample buffer. Thirty µl ACD was added to the PRP samples before platelets were separated by centrifugation (2000 × g, 10 min); 450 µl supernatant was taken and mixed in 225 µl 3× non-reduced sample buffer. The rest of the supernatant was discarded. Platelet pellet was then resuspended with HT buffer (in the presence of 10 ng/ml PGI2, pH 6.5) and spun down at 2000 × g for 10 min. Finally, the platelet pellet was resuspended in 40 µl 3× non-reduced sample buffer.

Protease–TaSER complex formation on platelet surface was evaluated by western blotting.

2.9 | Perfusion

2.9.1 | Platelet adhesion to VWF

Glass coverslips (24 × 50 mm) were incubated overnight in chromo-sulfuric acid and rinsed with distilled H_2O three times before placing in a 65°C stove for 15 min. They were subsequently incubated with 10 µg/ml VWF in HT buffer (pH 7.4; 1.5 h, RT) and blocked with 1% HSA in HT buffer for 30 min. Coverslips were attached to a perfusion chamber as described.[12] Citrated blood was spiked with the constructs (200 nM) or HT buffer (pH 7.4) and 10 µg/ml Acridine Orange for 5 min, before the start of the perfusion. This was perfused over pre-coated glass coverslips in a parallel–plate flow chamber at a shear rate of 800 s^{-1} for 9 min at RT. Platelet adhesion was recorded by real–time microscopy, using a Zeiss Z1 observer microscope equipped with a Zeiss filter set 10 and a Colibri light source with 470 nm LED, and ZEN 2 Pro software at a framerate of 0.2 frames/s. Images were analyzed for the area of platelet aggregates via Acridine Orange signal by the Image Analysis module within the ZEN 2 Pro software. After the perfusion, the chamber was rinsed with HT buffer (pH 7.4) and z-stack images were taken (1 µm/image) to evaluate platelet adhesion height by ZEN 2 Pro software.

2.9.2 | Aggregation formation on collagen

Glass coverslips, chamber preparation, and the perfusion were done as described in the previous section except that the glasses were coated with Horm collagen (100 µg/ml) instead of VWF.

2.9.3 | Fibrin formation on collagen

Coverslips were prepared as above and coated with 100 µg/ml Horm collagen +0.2 nM TF. Inlet tubing was blocked with 1% HSA in HT buffer for 5 min. Citrated blood (+1.5 µM CTI) was pre-incubated (5 min) with constructs (200 nM) or HT buffer (pH 7.4) and 90 µM of Alexa488-conjugated active-site-inhibited tissue plasminogen activator (tPA-Alexa488).[13] Instantly prior to the perfusion, 6.6 mM $CaCl_2$ and 3.03 $MgCl_2$ in HBS buffer (pH 7.4) were added to the blood. This was perfused over pre-coated glass coverslips in a parallel–plate flow chamber at a wall shear rate of 800 s^{-1} for 8 min at RT. Fibrin formation was observed and recorded by real-time microscopy using a Zeiss Z1 observer microscope equipped with a Zeiss filter set 10 and a Colibri light source with 470 nm LED, and ZEN 2 Pro software. Alexa488 and DIC Images were recorded at a framerate of 0.2 frames/sec. Movies were analyzed for the amount of fibrin via Alexa488 signal by the Image Analysis module within the ZEN 2 Pro

software. After perfusions, z-stack images were taken (1 μm/image) to evaluate fibrin mesh height and thrombus height.

2.10 | Data analysis

Statistical analyses were performed using Mann-Whitney U test. $P < .05$ was considered significant. All data analyses were performed with GraphPad Prism 7.0 (GraphPad Software).

3 | RESULTS

3.1 | TaSER design

Using phage display, we previously selected a V_HH against GPIbα.[14] We recombinantly fused this V_HH via a Gly/Ser-linker to α1AT-AIAR (graphically represented in Figure 1A; general properties in Table S2; protein expression in Figure S1) and expressed in HEK293 Freestyle cells. We named the resulting compound TaSER.

As controls, we produced: (1) non-targeting α1AT-AIAR, fused to a negative control V_HH (neg-AIAR); (2) α1AT-AIAR without a fused V_HH (α1AT-AIAR); (3) wild-type α1AT, fused to the V_HH that targets GPIbα (GPIbα-WT); and (4) wild-type α1AT, fused to a negative control V_HH (neg-WT).

We set out to examine whether the fusion of a V_HH influences the inhibitory function of the SERPIN moiety. Both TaSER and neg-AIAR dose-dependently inhibited thrombin similar to α1AT-AIAR while GPIbα-WT and neg-WT did not (Figure 1B). In plasma, TaSER, neg-AIAR, and α1AT-AIAR dose-dependently decreased tissue factor (TF)-driven thrombin formation (Figure 1C,D). As expected, GPIbα-WT and neg-WT did not impact thrombin generation. These experiments show that fusing a V_HH to α1AT-AIAR leaves its SERPIN function intact.

3.2 | TaSER binds to platelets and disrupts platelet agglutination.

Next, we set out to characterize TaSER platelet binding. We incubated PRP with TaSER or controls and pelleted the platelets by centrifugation. Western blots revealed that both GPIbα-targeting SERPINs, TaSER, and GPIbα-WT were dose-dependently enriched in the platelet pellet (Figure 2A; quantification in Figure 2B). In flow cytometry experiments, both TaSER and GPIbα-WT selectively and dose-dependently bound to platelets (Figure 2C). We subsequently investigated by FACS whether this binding impacts ristocetin-triggered VWF binding to platelet GPIbα in diluted whole blood (1:6). Both TaSER and GPIbα-WT selectively and dose-dependently inhibited platelet VWF binding (Figure 2D). The separate GPIbα-targeting V_HH, as well as an in-house–produced His- and Myc-tagged Caplacizumab variant (from here on indicated as Caplacizumab*[15];) blocked VWF binding with similar efficiency (Figure S2). Finally, TaSER and GPIbα-WT (600 nM) both disrupted preformed platelet
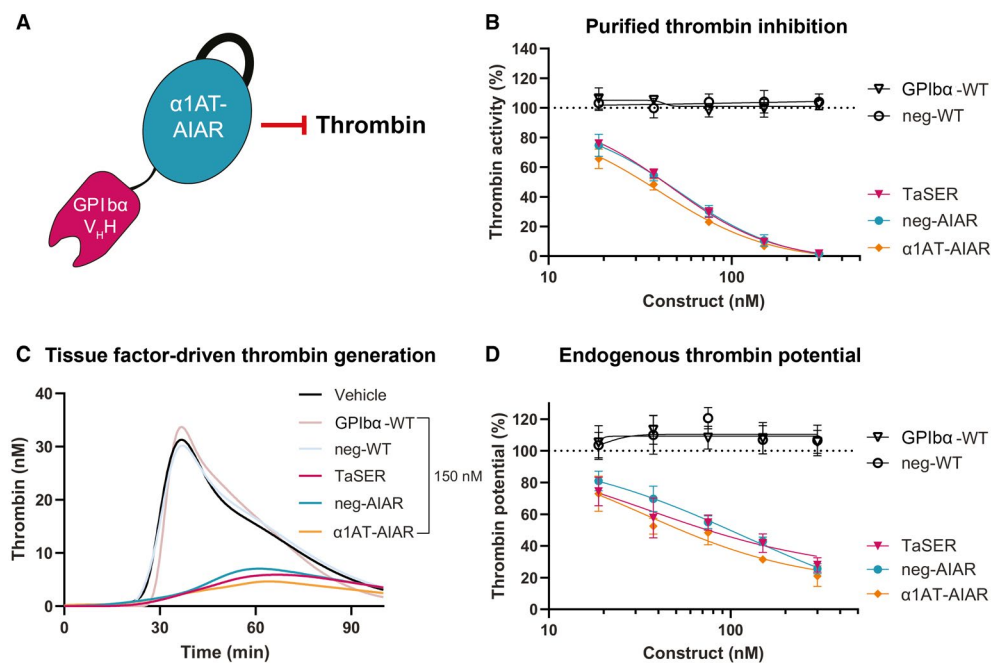

FIGURE 1 TaSER design and SERPIN properties. A, TaSER is a fusion protein consisting of an α1-antitrypsin variant ([355]AIAR[358]; α1AT-AIAR) that inhibits thrombin, fused with a GPIbα-targeting V_HH through a glycine-serine linker sequence. B, TaSER dose-dependently inhibits thrombin activity. C and D, Tissue factor-driven (0.1 pM) thrombin generation in normal pooled platelet-poor plasma. C, Representative TF-driven thrombogram in the presence of 150 nM TaSER or control constructs. D, TaSER dose-dependently decreases endogenous thrombin potential. Data represent the mean ± standard deviation of three separate experiments, each performed in duplicate. GPIbα, glycoprotein Ibα; SERPIN, serine protease inhibitor; TaSER, thrombin-inhibiting serine protease inhibitor; WT, wild type
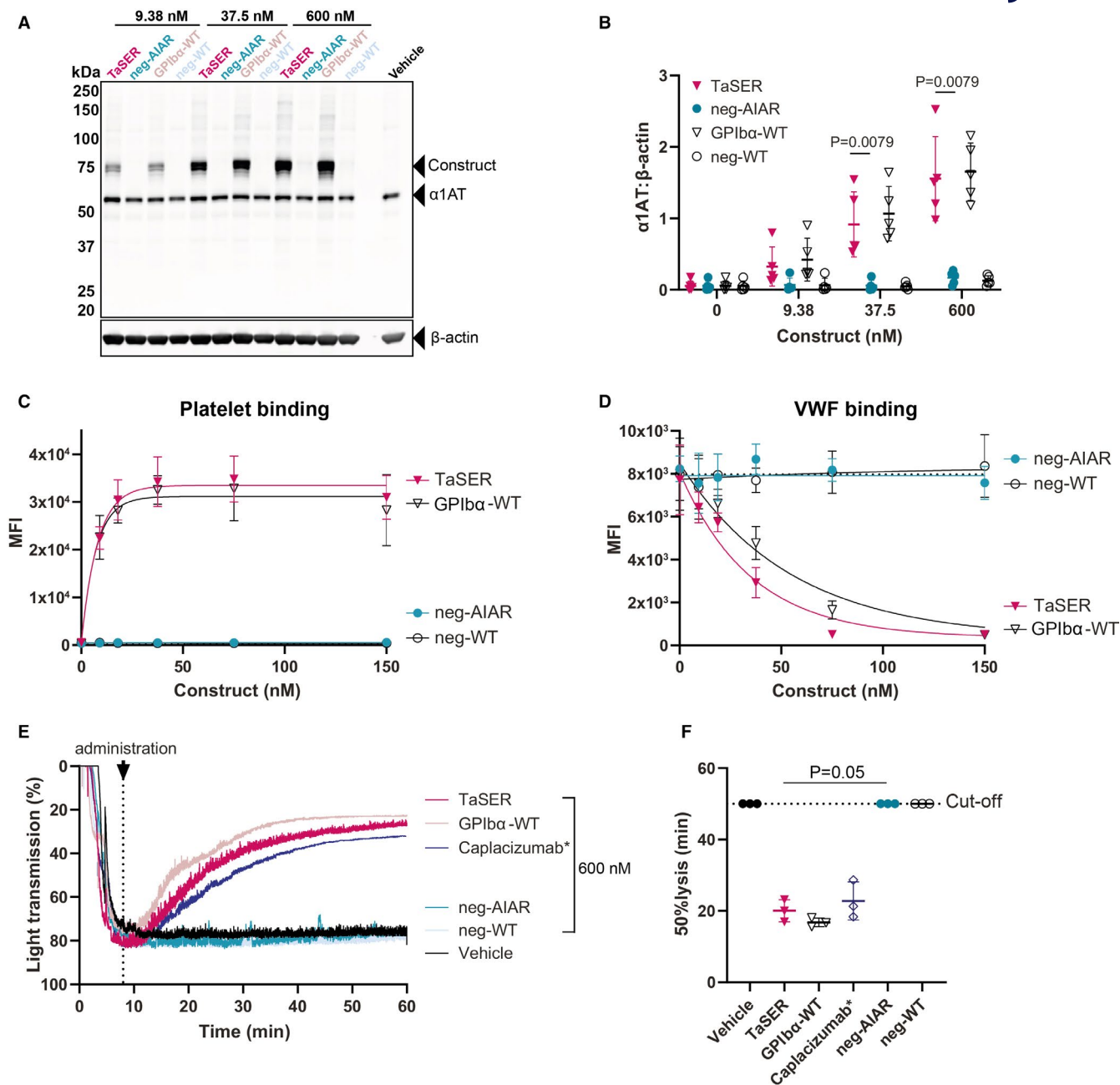
FIGURE 2 Thrombin-inhibiting serine protease inhibitor (TaSER) binds to platelets and disrupts platelet agglutination through von Willebrand factor (VWF) displacement. A–D, TaSER dose-dependently binds to platelets. A, Platelet-rich plasma was incubated with constructs, which were pelleted by centrifugation. Pellets were analyzed by western blot for the presence of the construct. B, Densitometric quantification of platelet binding of the constructs. Data represent the mean ± standard deviation (SD) of five separate experiments. TaSER binding was compared to neg-AIAR by Mann-Whitney *U* test. C, Median fluorescence intensity (MFI) of α1AT on platelets. Isolated platelets were incubated with the construct, which were pelleted by centrifugation. Pellets were analyzed by flow cytometry for the presence of the constructs. D, MFI of VWF in the presence of the construct. Flow cytometry showed VWF competitive binding by TaSER. Whole blood (1:6 diluted) was incubated with the construct in the presence of 200 μM ristocetin. Pellets were separated by centrifugation and analyzed by flow cytometry for the presence of VWF. E, Disruption of ristocetin-induced platelet agglutination by TaSER. Platelet agglutination was stimulated by addition of 0.6 mg/ml ristocetin for 6 min, after which 600 nM construct was added. The formation and disruption of agglutination were measured via light transmission. F, Time to reach 50% agglutinate lysis after construct administration. Data represent the mean ± SD of three separate experiments. TaSER was compared to neg-AIAR by Mann-Whitney *U* test

agglutinates with an efficiency that is comparable to Caplacizumab* (Figure 2E,F). In contrast, neg-AIAR and neg-WT could not disassemble platelet agglutinates.

3.3 | The platelet-targeting property of TaSER enhances SERPIN function.

Platelet activation is accompanied by degranulation and ATP release. Furthermore, platelets stimulate thrombin generation through phosphatidylserine exposure.[16]

We first assessed platelet-dependent thrombin generation in PRP and used a low TF concentration (0.1 pM) as trigger (Figure 3A–D). We found that TaSER reduces endogenous thrombin potential (ETP) 1.7 times more efficiently than neg-AIAR (IC_{50} = 78.9 ± 36.0 and 136.1 ± 38.1 nM respectively, P < .0429; Figure 3D). As expected, GPIbα-WT and neg-WT did not influence thrombin generation as wild-type α1AT does not inhibit thrombin.[9]

Next, we activated platelets with thrombin (0.9 U/ml) and determined expression of the activation marker P-selectin (indicates α-granule release) by FACS (Figure 3E). TaSER did not significantly prevent P-selectin expression compared to neg-AIAR (IC_{50} = 112.5 ± 33.6 and 153.2 ± 37.2 nM respectively, Figure 3F). Furthermore, both TaSER and neg-AIAR dose-dependently delayed platelet ATP secretion in whole blood (Figure 3G,H; trigger: 0.1 pM TF +5 mM $CaCl_2$). As before, GPIbα-WT and neg-WT did not influence platelet ATP secretion. Together, these data indicate that platelet targeting enhances the capacity of α1AT-AIAR to inhibit thrombin that is locally generated.

3.4 | TaSER complexes with thrombin on the platelet surface

SERPINs inhibit target proteases by forming stable covalent complexes, leading to a shift in apparent molecular weight when analyzed by SDS-PAGE.[17] We set out to investigate complex formation between TaSER and thrombin on the platelet surface. We added constructs to PRP and subsequently triggered thrombin generation (0.1 pM TF, 8 mM GPRP to prevent fibrin polymerization). After 90 min, platelets were pelleted, washed, and analyzed by western blot (Figure 4). Both TaSER and GPIbα-WT were enriched

in the platelet pellet (~72 kDa; Figure 2A). However, TaSER was predominantly detected as a ~109 kDa product, suggesting complex formation between TaSER (72 kDa) and thrombin (~37 kDa). After re-probing, this same band was found cross-reactive for thrombin (Figure 4A; quantification in Figure 4B). In the absence of $CaCl_2$, TaSER did not form these 109 kDa complexes (Figure S3). Together, these experiments indicate that TaSER inhibits thrombin in proximity to GPIbα.

3.5 | TaSER reduces platelet aggregation and fibrin formation under flow

We so far investigated the effect of TaSER under static conditions. We next investigated the impact of TaSER on key steps of thrombus formation in whole blood under laminar flow (shear rate 800 s^{-1}).

We perfused citrated whole blood in the absence or presence of constructs over VWF-coated or a collagen-coated cover slides and assessed platelet adhesion and platelet aggregation.

We found that TaSER and constructs with a GPIbα-targeting moiety (200 nM) significantly reduced platelet adhesion to VWF and aggregate formation on collagen (Figure 5A,B and Figure S4A-F). These data confirm that the GPIbα-targeting moiety of TaSER not only delivers SERPIN to platelets but also interferes with the role of VWF during platelet adhesion and aggregation.

Finally, we studied the effect of TaSER on fibrin formation. Recalcified whole blood spiked with constructs was perfused over collagen- and TF-coated cover slides. Fibrin formation was recorded by real-time fluorescence microscopy (Figure 5C–H, Video S1, and Figure S4G–L). In the presence of vehicle, fibrin formation started (defined as 10% of maximal fluorescence intensity) at ~2.6 min after onset of perfusion and the fibrin meshwork continued to grow up until 8 min (full occlusion of the flow system). Despite TaSER and neg-AIAR both being thrombin inhibitors in solution, only TaSER effectively slowed down fibrin formation under flow (TaSER; 7.0 ± 1.2 vs. neg-AIAR; 2.6 ± 0.1 min) when investigated at the same concentration (200 nM). Moreover, both thrombus height (55% reduction; Figure 5G) and fibrin deposition (75% reduction in mean fluorescence intensity; Figure 5H) were strongly decreased in the presence of TaSER, compared to neg-AIAR. In further flow experiments, we found that neg-AIAR was ineffective at 200 and 400 nM, but slowed down fibrin formation at higher concentrations (800 and

FIGURE 3 Thrombin-inhibiting serine protease inhibitor (TaSER) delays thrombin generation and platelet activation. A–D, Tissue factor (0.1 pM) induced thrombin generation in platelet-rich plasma (1.5 μM corn trypsin inhibitor [CTI]). A, Representative thrombogram in the presence of 75 nM of the construct. TaSER dose-dependently prolongs thrombin generation lag time (B) and diminishes thrombin potential (C). D, IC50 (i.e., concentration that reduced 50% of thrombin potential) of TaSER versus neg-AIAR. Data represent the mean ± standard deviation (SD) of four separate experiments, each performed in duplicate, analyzed by Mann-Whitney U test. E and F, TaSER dose-dependently inhibits platelet activation. E, Flow cytometry on activated platelets from isolated platelets stimulated by 0.9 U/ml thrombin in the presence of construct (9.38–600 nM). F, IC50 (i.e., concentration that reduced 50% of activated platelet) of TaSER versus neg-AIAR. Data represent the mean ± SD of three separate experiments, each performed in duplicate, analyzed by Mann-Whitney U test. n.s.: not significant. G and H, TaSER delays platelet ATP secretion in whole blood with higher efficacy than non-targeted α1AT-AIAR. G, Kinetic measurement of luciferin conversion. The construct (4.69–600 nM) was incubated with whole blood (1.5 μM CTI). Platelet activation was initiated by addition of 0.1 pM tissue factor and 5 mM CaCl2. H, TaSER delays ATP secretion

A Platelet-dependent thrombin generation
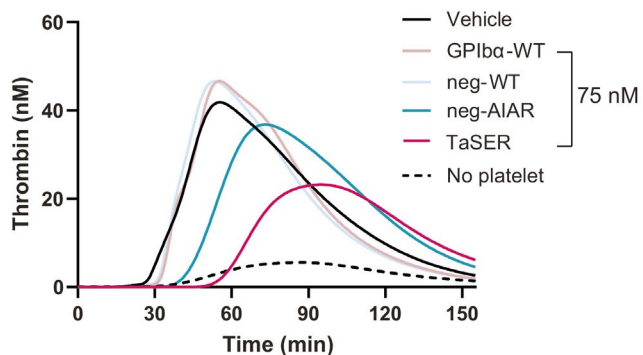
B Lag time
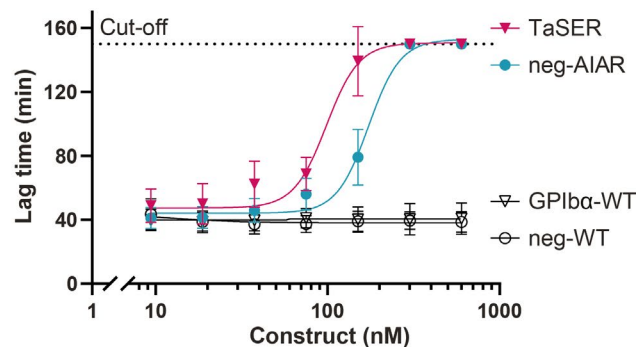
C Endogenous thrombin potential

D
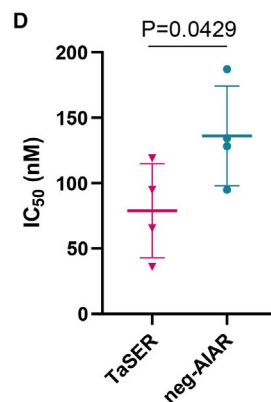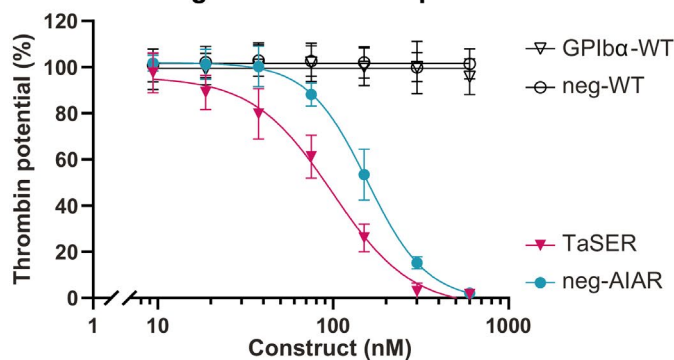
E Platelet activation (P-selectin expression)

F
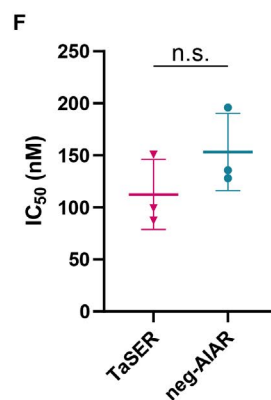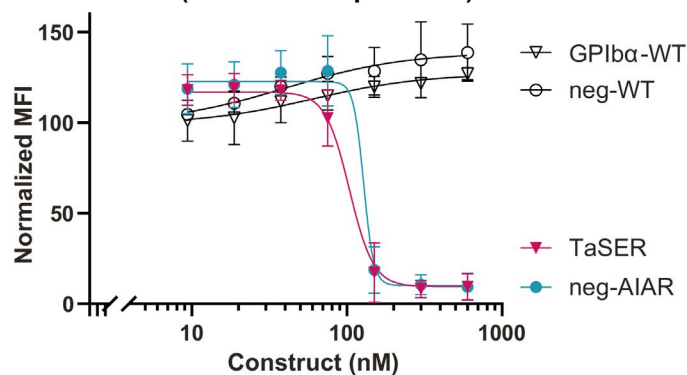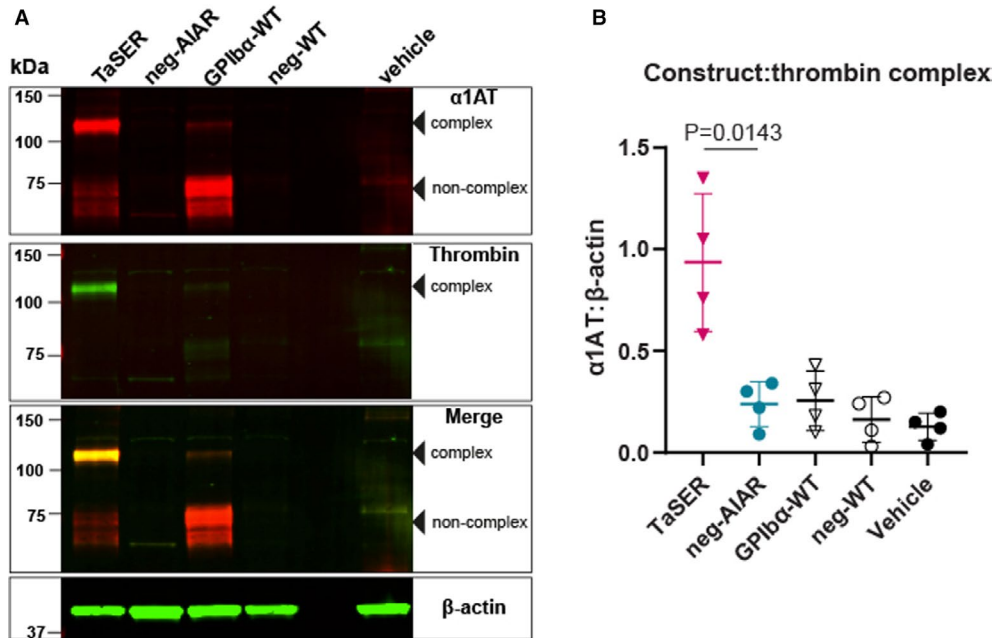
G ATP secretion
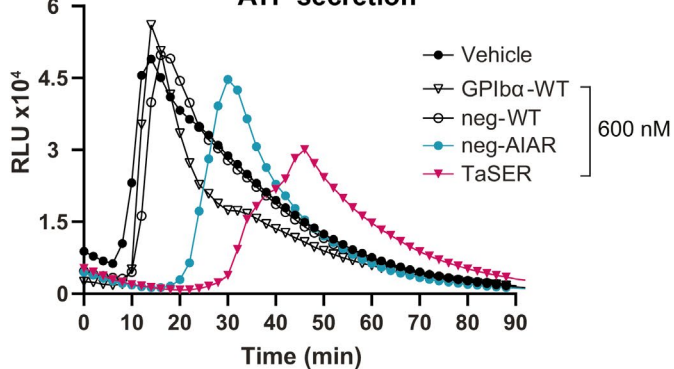
H Lag time
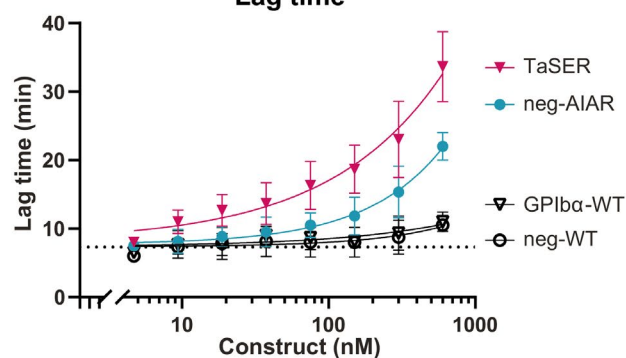
FIGURE 4 Thrombin-inhibiting serine protease inhibitor (TaSER) localizes on the platelet surface and forms complexes with thrombin. A, Western blot analysis (non-reducing) shows TaSER and GPIbα-WT (~72 kDa) in platelet pellet samples and complex formation (~109 kDa) with thrombin (expected size 37 kDa); 150 nM construct or vehicle was incubated in platelet-rich plasma (0.1 pM tissue factor and 1.5 µM corn trypsin inhibitor). Coagulation was initiated by adding 16.67 mM CaCl2. After 90 min incubation at 37°C, platelets were separated by centrifugation. B, Densitometric quantification of construct:thrombin complex. Data represent the mean ± standard deviation of four separate experiments analyzed by Mann-Whitney *U* test

1600 nM), although not to the same extent as 200 nM TaSER (Figure S5). These data demonstrate the antithrombotic benefit of targeting a thrombin-inhibiting SERPIN to platelets during thrombus formation in flowing blood.
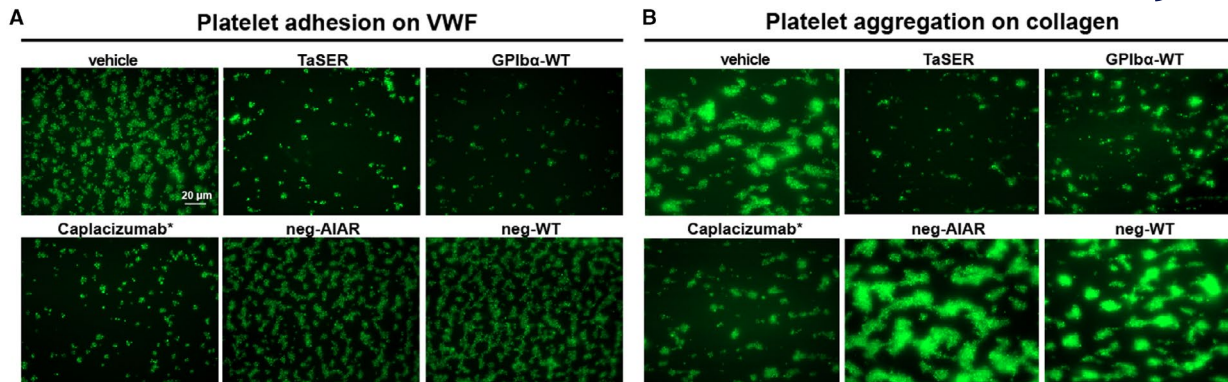
4 | DISCUSSION

The most commonly used approach to improve SERPIN function is through reactive center loop (RCL) modification.[7,18] Recent studies demonstrated the potential of RCL modified SERPIN *in vivo* models for hemophilia and contact system-driven thromboinflammation, respectively.[9,19] There are alternative ways to improve SERPIN properties. For example, SERPIN glycoengineering and PEGylation have been applied to increase SERPIN circulation half-life,[20–23] while SERPIN stability can be increased through backbone modification.[24] Furthermore, Sutherland et al. fused the N-terminal acidic
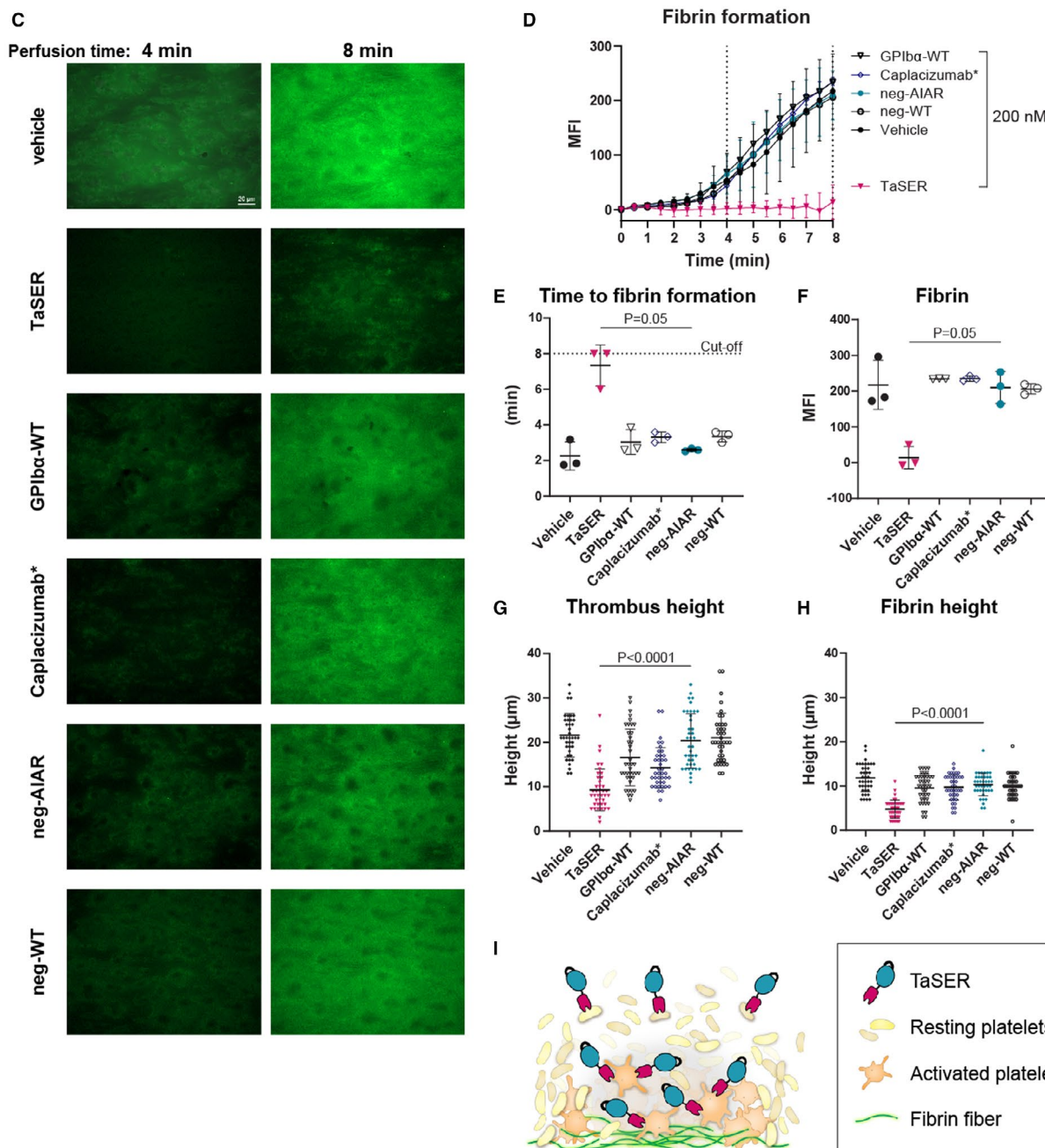
extension of heparin cofactor II (binds thrombin exosite 1) to the N-terminus of α1AT Pittsburgh (M358R). This innovative fusion protein increases the rate of thrombin inhibition with increased specificity.[25]

Many important biological processes driven by serine proteases take place on the cell surface and circulating SERPINs have to meet their target "by chance." In some situations, protease inactivation by SERPINs is influenced by the local environment, making target proteases hard to reach. This, for example, is the case for endothelial cells that keep C1-esterase inhibitor (an inhibitor of contact system and complement proteases) away through electrostatic repulsion.[26,27] In a growing thrombus, coagulation proteases (including thrombin) are physically protected from SERPIN inhibition because of its architecture. The thrombus core contains densely packed activated platelets in a fibrin network, and therefore is inaccessible to plasma protein exchange, while its shell is composed of minimally activated (P-selectin negative) platelets.[4,28]

FIGURE 5 Thrombin-inhibiting serine protease inhibitor (TaSER) limits platelet adhesion on von Willebrand factor (VWF), aggregate formation on collagen and fibrin formation on collagen and tissue factor (TF) under flow in whole blood. A, Platelet adhesion on VWF in the presence of 200 nM constructs after 9 min of the perfusion. Platelets were labeled with Acridine Orange (green). B, Platelet aggregation on collagen in the presence of 200 nM constructs at 9 min after the perfusion. Platelets were labeled with Acridine Orange (green). C, Fibrin formation in the presence of the 200 nM constructs at 4 and 8 min after the perfusion of whole blood over collagen and TF surface (shear rate 800 s^{-1}). Fibrin was visualized by Alexa488 fluorescence signal (green). D, Mean fluorescence intensity (MFI) of Alexa488 signal (fibrin). E, Initiation of fibrin formation (defined as 10% of maximal MFI).. F, Amount of fibrin at 8 min after the perfusion analyzed by MFI of Alexa488 signal. G, Z-stack images (1 µm/image) were evaluated for thrombus height via DIC. H, Z-stack images (1 µm/image) were evaluated for fibrin height via Alexa488 signal. I, Graphical representation of TaSER's proposed mechanism of action. Data represent the mean ± standard deviation of three separate experiments. TaSER was compared to neg-AIAR by Mann-Whitney *U* test

A **Platelet adhesion on VWF**

vehicle　　TaSER　　GPIbα-WT

Caplacizumab*　　neg-AIAR　　neg-WT

20 µm

B **Platelet aggregation on collagen**

vehicle　　TaSER　　GPIbα-WT

Caplacizumab*　　neg-AIAR　　neg-WT

Fibrin formation on collagen and TF

C

Perfusion time:　4 min　　8 min

vehicle

TaSER

GPIbα-WT

Caplacizumab*

neg-AIAR

neg-WT

20 µm

D **Fibrin formation**

MFI

Time (min)

GPIbα-WT
Caplacizumab*
neg-AIAR
neg-WT
Vehicle

TaSER

200 nM

E **Time to fibrin formation**

(min)

P=0.05

Cut-off

Vehicle, TaSER, GPIbα-WT, Caplacizumab*, neg-AIAR, neg-WT

F **Fibrin**

MFI

P=0.05

Vehicle, TaSER, GPIbα-WT, Caplacizumab*, neg-AIAR, neg-WT

G **Thrombus height**

Height (µm)

P<0.0001

Vehicle, TaSER, GPIbα-WT, Caplacizumab*, neg-AIAR, neg-WT

H **Fibrin height**

Height (µm)

P<0.0001

Vehicle, TaSER, GPIbα-WT, Caplacizumab*, neg-AIAR, neg-WT

I

TaSER

Resting platelets

Activated platelet

Fibrin fiber

In this study, we hypothesized that targeting a SERPIN to its prospective site of action would enhance its inhibitory capacity. We aimed to design TaSER as an antithrombotic protein that restricts fibrin formation through incorporation into growing thrombi (Figure 5I).

We selected α1AT-AIAR as a model SERPIN. It (among others) is a capable, but not extremely powerful, thrombin inhibitor (k_2: 5.5×10^4 M^{-1} s^{-1}) compared to antithrombin (k_2: 1.3–7.4 $\times 10^7$ M^{-1} s^{-1}, in the presence of heparin) or α1AT Pittsburgh (k_2: 3.1×10^5 M^{-1} s^{-1}).[9,29-31] We used this model SERPIN to explore the possible added value of targeted SERPIN delivery *in vitro*. For future preclinical investigation of targeted SERPIN delivery *in vivo*, selecting a more powerful SERPIN moiety should further increase its efficacy. Furthermore, there are modifications possible to improve the efficacy and specificity profile of future TaSER variants.[32]

We found that V_HH fusion to the SERPIN N-terminus (opposite the RCL) does not interfere with SERPIN in its function as a thrombin inhibitor (Figure 1). Through its VWF-displacing properties (Figure 2), the V_HH moiety interferes with thrombus build-up (Figure 5) and delivers α1AT-AIAR (Figure 4) to the thrombus like a "Trojan horse" for incorporation and protease inhibition. This further interferes with thrombus build-up by delaying fibrin formation much more efficiently than its non-targeting control variant (Figure S5). The lack of effect of non-targeting neg-AIAR suggests that it is unable to reach its target in our flow models. The limited effect of a GPIbα-targeting V_HH, fused to wild-type α1AT, shows that the disaggregating properties of this molecule are insufficient to delay fibrin formation. This finding is consistent with a previous study, showing that prevention of platelet accumulation had little effect on the thrombus fibrin formation after injury.[33] Our experiments show that the combined activities of TaSER enable it to act as an effective antithrombotic in our flow models for thrombosis.

Although full-length anti-GPIbα antibodies can induce thrombocytopenia,[34] the binding of TaSER's V_HH moiety is improbable to trigger platelet clearance as it lacks the required Fc tail. In contrast, we expect that TaSER assumes the circulating half-life of platelets after binding (7–10 days), which is much longer than the half-life of free recombinant α1AT *in vivo* (46.9 min in mice[21]). This fits the profile of an agent that can be used prophylactically in states where there is an expected temporarily increased thrombogenic state, for example, after elective orthopedic surgery. The dose that is effective and safe will have to be determined *in vivo*, but can be monitored with *in vitro* assays (e.g., platelet-dependent thrombin generation).

Finally, we propose that the development of targeting SERPIN-based fusion proteins extends beyond the context of thrombosis. For example, by targeting SERPINs to the bacterial surface, it should be possible to interfere with serine-protease–driven virulence factors. In conclusion, the targeted delivery of SERPINs to desired sites of action should hold value for diverse therapeutic applications.

CONFLICTS OF INTEREST

M.R. is employed by Synapse Research Institute, which is a part of the Stago group that markets the Calibrated Automated Thrombography and ST-Genesia. W.S., S.S., A.D.B., N.D.v.K., H.E.O., M.Z, T.R., C.C.C, S.d.M, and C.M. declare no conflict of interest.

AUTHOR CONTRIBUTIONS

C.M. designed research; W.S., S.S., A.D.B., N.D.v.K., H.E.O., and M.Z. performed research; M.R. and T.R. contributed new reagents/analytic tools; W.S., C.C.C., S.d.M., and C.M. analyzed data; and W.S. and C.M. wrote the paper.

ORCID

Wariya Sanrattana https://orcid.org/0000-0002-8731-8673
Simone Smits https://orcid.org/0000-0002-3229-7238
Arjan D. Barendrecht https://orcid.org/0000-0002-0653-5538
Nadine D. van Kleef https://orcid.org/0000-0001-7162-9277
Hinde El Otmani https://orcid.org/0000-0002-2344-6027
Minka Zivkovic https://orcid.org/0000-0003-4545-7939
Mark Roest https://orcid.org/0000-0002-7349-7068
Thomas Renné https://orcid.org/0000-0003-4594-5975
Chantal C. Clark https://orcid.org/0000-0001-9614-7135
Steven de Maat https://orcid.org/0000-0003-1179-374X
Coen Maas https://orcid.org/0000-0003-4593-0976

REFERENCES

1. Flaumenhaft R. Thrombus formation reimagined. *Blood*. 2014;124:1697-1698.
2. Welsh JD, Stalker TJ, Voronov R, et al. A systems approach to hemostasis: 1. The interdependence of thrombus architecture and agonist movements in the gaps between platelets. *Blood*. 2014;124(11):1808-1815.
3. Tomaiuolo M, Stalker TJ, Welsh JD, Diamond SL, Sinno T, Brass LF. A systems approach to hemostasis: 2. Computational analysis of molecular transport in the thrombus microenvironment. *Blood*. 2014;124(11):1816-1823.
4. Stalker TJ, Traxler EA, Wu J, et al. Hierarchical organization in the hemostatic response and its relationship to the platelet-signaling network. *Blood*. 2013;121(10):1875-1885.
5. Di Meglio L, Desilles J-P, Ollivier V, et al. Acute ischemic stroke thrombi have an outer shell that impairs fibrinolysis. *Neurology*. 2019;93(18):e1686-e1698.
6. Sanrattana W, Maas C, de Maat S. SERPINs-From trap to treatment. *Front Med*. 2019;12(6):25.
7. Schapira M, Ramus MA, Waeber B, et al. Protection by recombinant alpha 1-antitrypsin Ala357 Arg358 against arterial hypotension induced by factor XII fragment. *J Clin Invest*. 1987;80(2):582-585.
8. Jallat S, Courtney MJ. Variants of alpha 1-antitrypsin which are useful, in particular, as kallikrein inhibitors. 1986.
9. De Maat S, Sanrattana W, Mailer RK, et al. Design and characterization of a1-antitrypsin variants for treatment of contact system-driven thromboinflammation. *Blood*. 2019;134(19):1658-1669.
10. de Maat S, Björkqvist J, Suffritti C, et al. Plasmin is a natural trigger for bradykinin production in patients with hereditary angioedema with factor XII mutations. *J Allergy Clin Immunol*. 2016;138(5):1414-1423.e9.

11. Hemker HC, Giesen P, Al Dieri R, et al. Calibrated automated thrombin generation measurement in clotting plasma. *Pathophysiol Haemost Thromb.* 2003;33(1):4-15.

12. Barendrecht AD, Verhoef JJF, Pignatelli S, Pasterkamp G, Heijnen HFG, Maas C. Live-cell imaging of platelet degranulation and secretion under flow. *J Vis Exp.* 2017;10(125):55658.

13. Yu Y, Gool E, Berckmans RJ, et al. Extracellular vesicles from human saliva promote hemostasis by delivering coagulant tissue factor to activated platelets. *J Thromb Haemost.* 2018;16(6):1153-1163.

14. van Asten I, Blaauwgeers M, Granneman L, et al. Flow cytometric mepacrine fluorescence can be used for the exclusion of platelet dense granule deficiency. *J Thromb Haemost.* 2020;18(3):706-713.

15. Peyvandi F, Scully M, Kremer Hovinga JA, et al. Caplacizumab for acquired thrombotic thrombocytopenic purpura. *N Engl J Med.* 2016;374(6):511-522.

16. van der Meijden PEJ, Heemskerk JWM. Platelet biology and functions: new concepts and clinical perspectives. *Nat Rev Cardiol.* 2019;16(3):166-179.

17. Gettins PGW. Serpin structure, mechanism, and function. *Chem Rev.* 2002;102(12):4751-4804.

18. Sulikowski T, Bauer BA, Patston PA. α1-Proteinase inhibitor mutants with specificity for plasma kallikrein and C1s but not C1. *Protein Sci.* 2009;11(9):2230-2236.

19. Polderdijk SGI, Adams TE, Ivanciu L, Camire RM, Baglin TP, Huntington JA. Design and characterization of an APC-specific serpin for the treatment of hemophilia. *Blood.* 2017;129(1):105-113.

20. Lindhout T, Iqbal U, Willis LM, et al. Site-specific enzymatic polysialylation of therapeutic proteins using bacterial enzymes. *Proc Natl Acad Sci USA.* 2011;108(18):7397-7402.

21. Lusch A, Kaup M, Marx U, Tauber R, Blanchard V, Berger M. Development and analysis of alpha 1-antitrypsin neoglycoproteins: The impact of additional N-glycosylation sites on serum half-life. *Mol Pharm.* 2013;10(7):2216-2229.

22. Chung HS, Kim JS, Lee SM, Park SJ. Additional N-glycosylation in the N-terminal region of recombinant human alpha-1 antitrypsin enhances the circulatory half-life in Sprague-Dawley rats. *Glycoconj J.* 2016;33(2):201-208.

23. Cantin AM, Woods DE, Cloutier D, Dufour EK, Leduc R. Polyethylene glycol conjugation at Cys232 prolongs the half-life of α1 Proteinase inhibitor. *Am J Respir Cell Mol Biol.* 2002;27(6):659-665.

24. Porebski BT, Keleher S, Hollins JJ, et al. Smoothing a rugged protein folding landscape by sequence-based redesign. *Sci Rep.* 2016;6:33958.

25. Sutherland JS, Bhakta V, Filion ML, Sheffield WP. The transferable tail: fusion of the N-terminal acidic extension of heparin cofactor II to α1-proteinase inhibitor M358R specifically increases the rate of thrombin inhibition. *Biochemistry.* 2006;45(38):11444-11452.

26. Pixley RA, Schmaier A, Colman RW. Effect of negatively charged activating compounds on inactivation of factor XIIa by C$\bar{\text{I}}$ inhibitor. *Arch Biochem Biophys.* 1987;256(2):490-498.

27. Ravindran S, Grys TE, Welch RA, Schapira M, Patston PA. Inhibition of plasma kallikrein by CI-inhibitor: role of endothelial cells and the amino-terminal domain of CI-inhibitor. *Thromb Haemost.* 2004;92(6):1277-1283.

28. Tomaiuolo M, Matzko CN, Poventud-Fuentes I, Weisel JW, Brass LF, Stalker TJ. Interrelationships between structure and function during the hemostatic response to injury. *Proc Natl Acad Sci USA.* 2019;116(6):2243-2252.

29. Lewis J, Iammarino R, Spero J, Hasiba U. Antithrombin Pittsburgh: an alpha1-antitrypsin variant causing hemorrhagic disease. *Blood.* 1978;51(1):129-137.

30. Olson ST, Björk I. Predominant contribution of surface approximation to the mechanism of heparin acceleration of the antithrombin-thrombin reaction: elucidation from salt concentration effects. *J Biol Chem.* 1991;266(10):6353-6364.

31. Beeler D, Rosenberg R, Jordan R. Fractionation of low molecular weight heparin species and their interaction with antithrombin. *J Biol Chem.* 1979;254(8):2902-2913.

32. Sanrattana W, Smits S, Monroe D, Maas C, de Maat S. A novel prediction platform to enhance the design of therapeutic SERPINs [abstract]. *Res Pract Thromb Haemost.* 2020;4(Suppl 1). https://abstracts.isth.org/abstract/a-novel-prediction-platform-to-enhance-the-design-of-therapeutic-serpins/. Accessed October 25, 2021.

33. Ivanciu L, Krishnaswamy S, Camire RM. New insights into the spatiotemporal localization of prothrombinase in vivo. *Blood.* 2014;124(11):1705-1714.

34. Morodomi Y, Kanaji S, Won E, Ruggeri ZM, Kanaji T. Mechanisms of anti-GPIbα antibody-induced thrombocytopenia in mice. *Blood.* 2020;135(25):2292-2301.

SUPPORTING INFORMATION

Additional supporting information may be found in the online version of the article at the publisher's website.